Electronic Supplementary Information (ESI) for

Multiscale pore contained carbon nanofiber-based field-effect-transistor biosensor for nesfatin-1 detection

Sung Gun Kim[a] *and Jun Seop Lee*[b*]

[a]Samsung Electronics, San #16 Banwol-Dong, Hwasung, Gyeonggi-Do18448, South Korea

[b]Department of Materials Science and Engineering, Gachon University, 1342 Seongnam-Daero, Sujeong-Gu, Seongnam-Si, Gyeonggi-Do 13120, Republic of Korea

Corresponding Author:

*E-mail: (J.S. Lee) junseop@gachon.ac.kr; Tel.: +82-31-750-5814; Fax: +82-31-750-5389

1. Electrospinning mechanism of the polymer solution

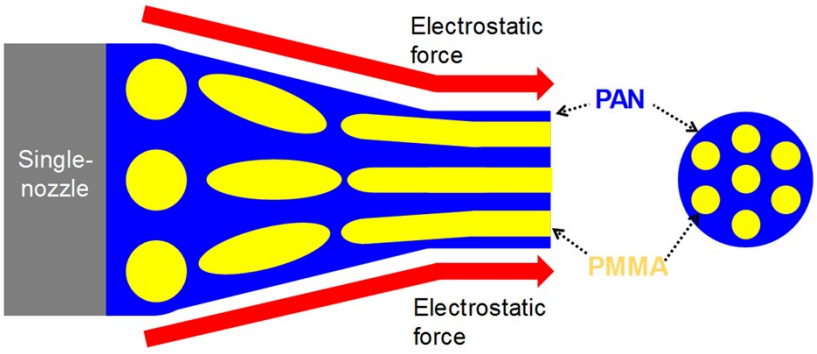

Figure S1. Mechanism of formation of the multicore-contained polymer nanofibers through single-nozzle co-electrospinning.

2. BET surface area and BJH pore distribution of CNFs

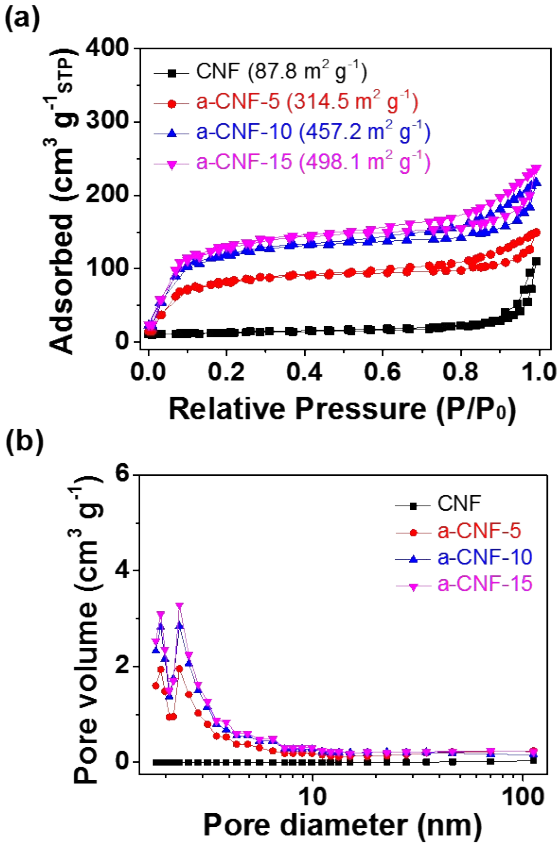

Figure S2. (a) Nitrogen adsorption-desorption and (b) pore size distribution curves of the CNFs with different activations time: 0 min (black); 5 min (red); 10 min (blue); 15 min (pink).

3. Comparison XPS C 1s spectra of a-MPCNFs

Table S1. Comparison of C 1s XPS spectra with different activation times.

	284.3 eV (C=C/C-C) [at%]	286.5 eV (C-O) [at%]	288.0 eV (C=O) [at%]	$I_{286.5}/I_{284.3}$	$I_{288.0}/I_{284.3}$
MPCNF	73	14.5	12.5	0.199	0.171
a-MPCNF-5	69	16	15	0.232	0.217
a-MPCNF-10	64	19.5	16.5	0.305	0.258
a-MPCNF-15	59	22	19	0.373	0.322

4. Morphology of Ab-a-CNF

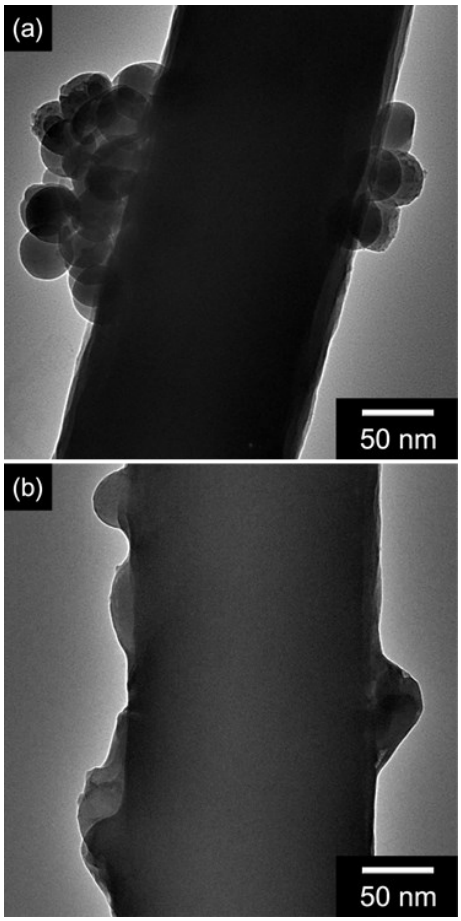

Figure S3. TEM images of anti-NES1 introduced CNFs (a) without and (b) after activation process.

5. C 1s XPS of Ab-a-MPCNF-10

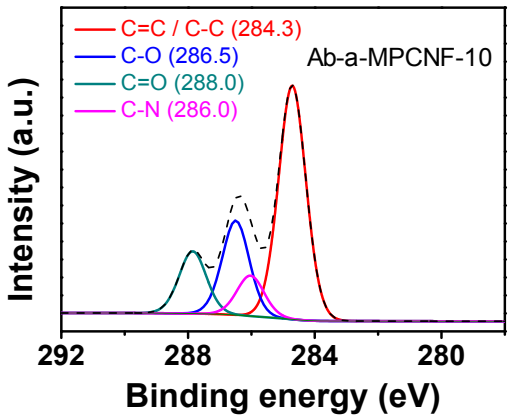

Figure S4. C 1s XPS spectra of a-MPCNF after immobilization of anti-NES1.

6. IV curve of a-CNF-10 based electrode

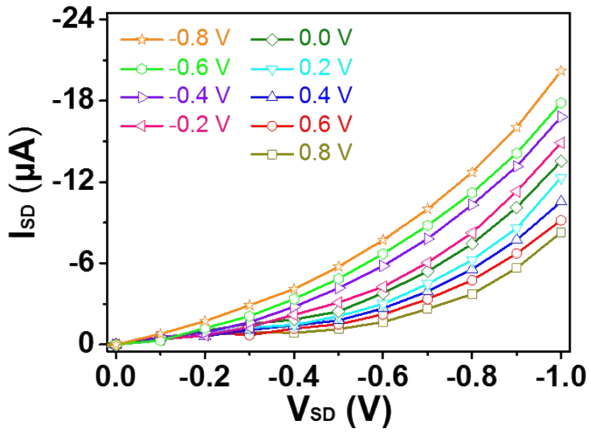

Figure S5. I_{SD}–V_{SD} characteristics of the Ab-a-CNF-based FET sensing electrode (−0.8 V ≤ V_G ≤ +0.8 V in steps of 0.2 V with a V_{SD} scan rate of 10 mV s^{-1}).

7. Real-time signal change in the NES1 response

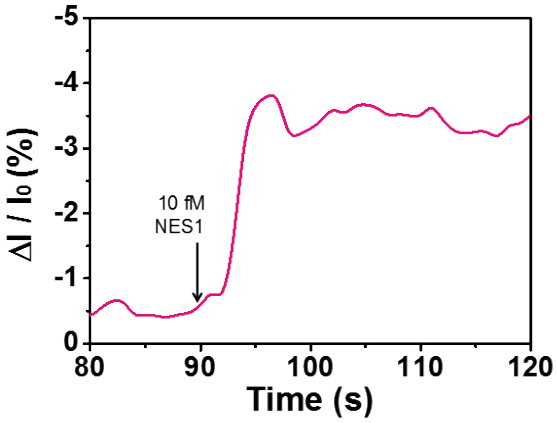

Figure S6. Saturation sensing signal of Ab-a-MPCNF electrode with 10 fM NES1 exposure.

8. Sensing performance of carbon-based nanomaterials

Table S2. Summary of representative carbon nanomaterial-based biosensor

Material	Receptor	Target Material	Sensing Principle	Linear range	Limit of detection	Ref.
Vertically aligned CNF	-	Dopamine	Electrochemical	-	50 nM	[S1]
PtNP-CNF/PDDA[1)]	Lactate Oxidase	H_2O_2	Amperometric	25 – 1500 μM	11 μM	[S2]
PANI/CNT	Binding aptamer	$VEGF_{165}$	Electrochemical	0.5 pg mL^{-1} – 1 μg mL^{-1}	0.4 pg mL^{-1}	[S3]
Ni-ZrO_2/MWCNT	-	5-amino salicylic acid	Electrochemical	0.001 – 500 μM	0.0029 μM	[S4]
LSG-NF[2)]-AgNPs	Binding aptamer	Tuberculosis	Electrochemical	1 fM – 1 nM	1 fM	[S5]
Th-Cs-Ni$(OH)_2$NPs-ERGO[3)]	p53-antigen	p53	Electrochemical	0.1 – 500 pg mL^{-1}	0.001 pg mL^{-1}	[S6]
a-MPCNF-10	NES1 antibody	NES1	FET	0.1 fM – 10 nM	0.1 fM	This work

[1)]PDDA: Poly(diallyldimethylammonium), [2)] Laser derived-graphene nanofiber, [3)]Thionine (as an electron transfer mediator)/chitosan /nickel hydroxide nanoparticles/electrochemically reduced graphene oxide

[S1] Biosensors and Bioelectronics 2013, 42, 434-438.

[S2] Biosensors and Bioelectronics 2014, 56, 345-351.

[S3] Biosensors 2021, 11, 114.

[S4] Analyst 2021, 146, 664.

[S5] Scientific Reports 2021, 11, 5475.

[S6] Talanta 2021, 230, 122276.

9. Selectivity test of the electrode among peptide hormones

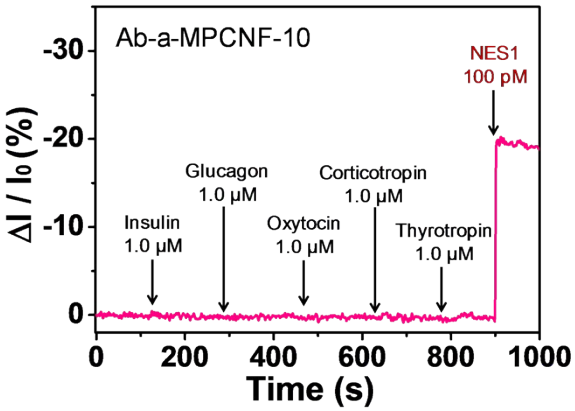

Figure S7. A real-time response of Ab-a-MPCNFs FET sensor to target (NES1) and non-target peptide hormones (insulin, glucagon, oxytocin, corticotropin, thyrotropin).

10. Sensing performance of Ab-a-CNF in an artificial saliva

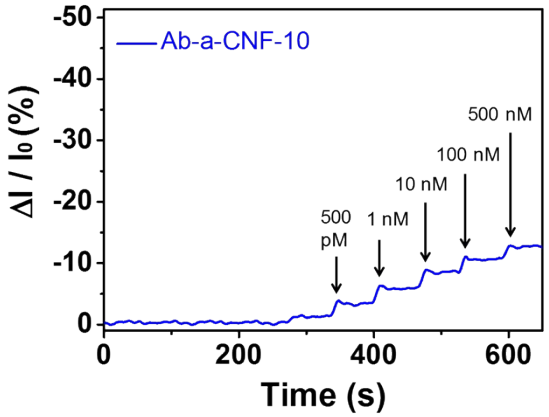

Figure S8. A real-time response of the normalized current of Ab-a-CNF sensor with various concentration of NES1 in artificial saliva solution.